

Received April 16, 2018, accepted May 31, 2018, date of publication June 12, 2018, date of current version July 12, 2018.

Digital Object Identifier 10.1109/ACCESS.2018.2843782

Compact Wideband Filtering Balun Using Stacked Composite Resonators

LIN-PING FENG^{ID} AND LEI ZHU^{ID}, (Fellow, IEEE)

Department of Electrical and Computer Engineering, Faculty of Science and Technology, University of Macau, Macau 999078, China

Corresponding author: Lei Zhu (leizhu@umac.mo)

This work was supported in part by the Macao Science and Technology Development Fund through FDCT Research under Grant 091/2016/A2, in part by the National Natural Science Foundation of China under Grant 61571468, and in part by the University of Macau through Multi-Year Research under Grants MYRG2017-00007-FST and CPG2017-00028-FST.

ABSTRACT In this paper, a direct synthesis method is proposed for design and exploration of wideband filtering balun based on a compact triple-mode stacked composite resonators. Accordingly, an equivalent physics-based non-redundant network is developed for interpreting its working mechanism and facilitating the whole design process. Based on the derived non-redundant model, a synthesis approach is then established and described to the efficient design of the proposed filtering balun according to the design specifications. As a result, all the circuit element values and dimensions are directly determined. A wideband filtering balun is then designed to confirm its performance and validate the effectiveness of the proposed synthesis method. In this aspect, a triple-mode wideband filtering balun prototype has been designed, fabricated, and measured. The synthesized, simulated, and measured results are found in good agreement with each other over a wide operating band range, and they have demonstrated the attractive performances of the proposed wideband filtering balun, such as wide bandwidth of operation, sharpened frequency selectivity, good magnitude imbalance, and phase difference.

INDEX TERMS Synthesis, filtering balun, triple-mode resonator, magnitude imbalance, phase imbalance difference.

I. INTRODUCTION

With advances of modern communication systems over the past few years, there is an irreversible trend that demands the next generation RF front-end module to be compact, lightweight, low cost, and multi-functional in today's wireless systems. To meet such an inevitable trend, the collaborative design of a few multi-functional circuits incorporating as a single circuit block with multi-functional property has shown promising potential in many practical applications. As depicted in Fig. 1(a) and (b), three cascaded circuit blocks, i.e., filter, line and balun, are incorporated as one single filtering balun block. In this collaborative design conception, the filtering balun can not only hold the feature of a balun in converting an unbalanced signal to a balanced one, but also achieve the desired frequency selectivity of a filter. Up to now, much great effort has been made in this area to accommodate this trend [1]–[18]. Nowadays, the Low Temperature Co-fired Ceramic technology (LTCC) technology has been widely employed for miniaturization of an entire RF front-end module. In [1]–[3], this technology has been successfully applied to design of balun bandpass filters (BPFs)

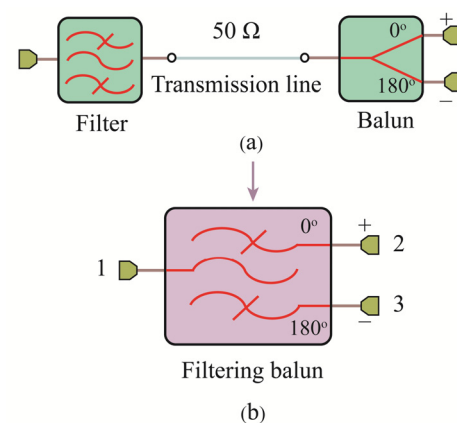


FIGURE 1. Schematics evolution of proposed compact UWB filtering balun. (a) Conventional one via cascaded filter, line and balun. (b) Proposed one via incorporating as a single circuit block.

or balun filters with significant size reduction, but it unfortunately increases cost and complicates process in fabrication. Recently, a variety of multilayer balun BPFs with compact

size and good filtering performance have been proposed in [4] and [5], but the complexity in geometrical structure and design procedure have limited its further practical application. In the past few years, the inherent antiphase property of a dual-mode resonator has been utilized in design of a class of balun BPFs [6]–[10], but these balun filters suffer from relative narrow operating bandwidth. Based on Marchand-type balun topology, an alternative class of dual-band and tri-band BPF baluns have been excogitated using the coupled-line topology [11], [12]. But, they are restricted with a narrow bandwidth. Apart from this, a half-wavelength resonator with desired out-of-phase signals has been successfully to constitute the bandpass filters by utilizing the inherent antiphase property as done in [13] and [14]. However, this type of balun filter still suffers from narrow bandwidth and needs to intricate circuit configuration. In [15], a hybrid resonator is introduced to build a bandpass balun filter with compact size and good filtering response, and its electrical performance is analyzed and designed by using the even- and odd-mode approach. Obviously, this approach is not suitable for wideband application.

To meet current wideband demand, much efforts has been focused on realization of a wideband BPF balun as reported in [16]–[18]. Although the work in [17] exhibits good filtering response, it fails to provide a systematic procedure for design of this wideband filtering balun with prescribed specifications. In [18], a wideband three-port balun BPF is reported with the desired bandpass response such as controllable fractional bandwidth (FBW), good selectivity, and extended stopband. Nevertheless, it suffers from extremely complicated geometry with the need of extra lumped element and via to ground, and many involved elements in design, thereby bringing out inconvenience in practical applications.

The primary motivation of this work is to propose a novel direct synthesis method for design of triple-mode wideband filtering balun using stacked composite resonators. The organization of this paper will be arranged as follows. In Section II, an equivalent non-redundant circuit network is introduced and developed for interpreting its working mechanism and facilitating the whole design process of this type of wideband filtering baluns. In Section III, a wideband filtering balun will be designed by the proposed synthesis method. Subsequently, a triple-mode wideband filtering balun will be designed, fabricated, and measured in Section IV. Lastly, Section V concludes this work.

II. ANALYSIS AND SYNTHESIS OF PROPOSED FILTERING BALUN

In this section, the entire circuit model of the proposed filtering wideband balun will be presented first and then simplified. A legitimate circuit transformation is applied to simplify the entire balun circuit into a non-redundant two-port network. Then, a synthesis approach is described to design this filtering balun according to design specifications.

A. EQUIVALENT MODEL OF A TRIPLE-MODE RESONATOR

Fig. 2(a) depicts a conceptual 3-D view of the basic structure of the proposed wideband triple-mode filtering balun, and Fig. 2(b) indicates the two scenarios of its cross-sectional views. The proposed triple-mode filtering balun consists of a $\lambda_g/4$ microstrip-line (MSL) open-circuited stub on the top of the upper substrate, a uniform $\lambda_g/2$ MSL resonator on the bottom of the lower substrate, and a $\lambda_g/2$ slotline resonator on the common ground plane. The working mechanism of the proposed wideband filtering balun can be explained by the concept of a triple-mode resonator with three resonant modes in the passband as is elaborated later on.

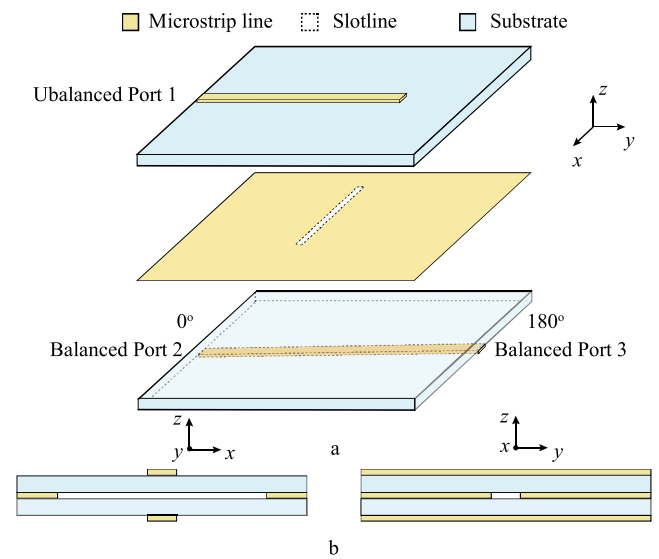


FIGURE 2. Basic physical scenarios of the proposed triple-mode UWB filtering balun (a) Three-dimensional view, (b) Cross-sectional views.

B. PHYSICS-BASED EQUIVALENT-CIRCUITS MODE

Fig. 3(a) indicates an equivalent distributed circuit model using transmission lines and ideal transformers. The distributed circuit is composed of one open-ended stub connected to input port (unbalanced port), two short-ended stubs, and one interconnecting uniform MSL connected to two output ports (balanced ports) with the impedances of Z_O , Z_C and Z_M , as well as three impedance transformers with the turn ratios of n_1 , n_2 , and n_3 , respectively. Physically, n_1 and n_2 represent the EM couplings between the slotline resonator and MSLs, respectively, while n_3 characterizes the couplings between open-ended stub and input microstrip line. The electrical lengths of all the stubs and uniform MSLs are set as $\lambda_g/4$ at central frequency. Since the balanced outputs and absorbing the transformer n_3 into the open stub, the two output ports can be combined into one port. Accordingly, its two-port distributed circuit network can be obtained as depicted in Fig. 3(b). Furthermore, based on the Richard's transformation [19], [20] as illustrated in Fig.4, the open-ended stub, short-ended stubs, and interconnecting MSLs are equivalently represented as the lumped capacitor, inductors,

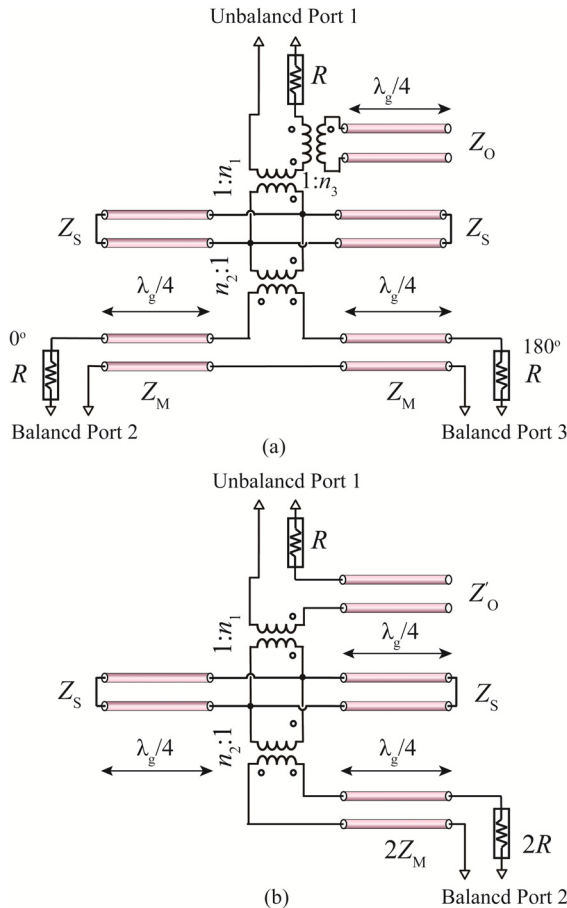


FIGURE 3. Equivalent circuit models of the proposed triple-mode filtering balun. (a) Initial three-port model. (b) Simplified two-port model.

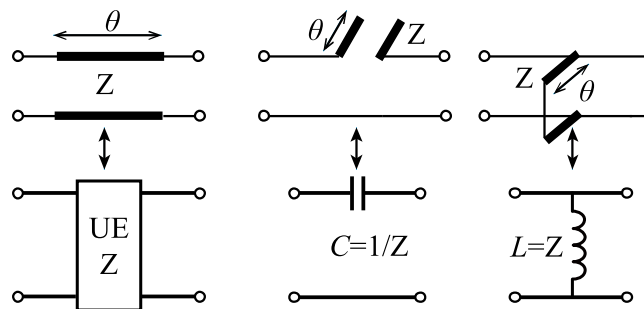


FIGURE 4. Equivalence of an interconnecting line, open-ended line, and short-ended line as their corresponding lumped-element UE, C and L elements, respectively, under the Richard's transformation.

and unit elements (UE), respectively. Thus, the lumped-element circuit prototype can be derived as shown Fig. 5(a).

As stated above, the following equations can be determined according to the lumped- and distributed-element relationship under the Richard's transformation in Fig. (4),

$$Z'_O = \frac{Z_O}{n_3^2} \quad (1)$$

$$C = 1/Z'_O \quad (2)$$

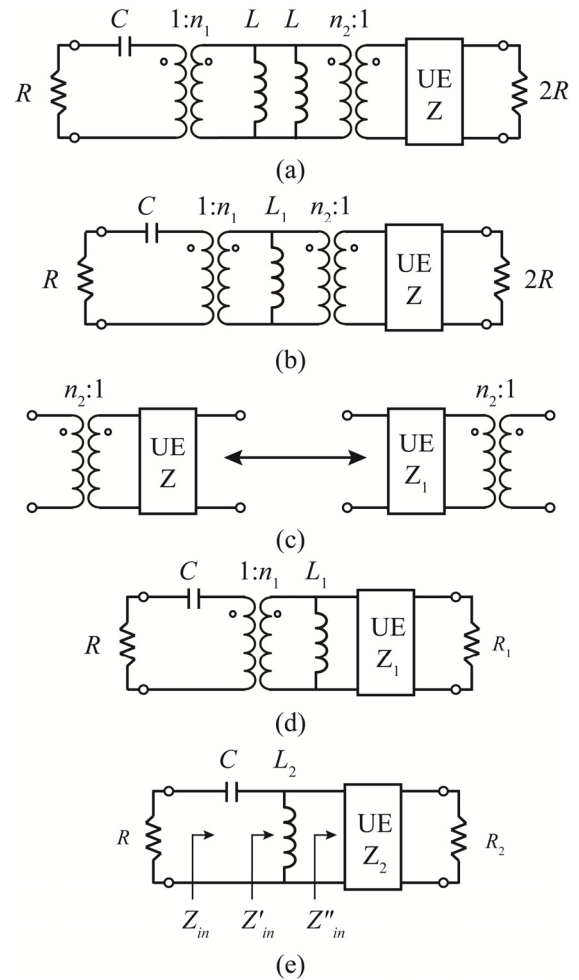


FIGURE 5. Schematics of equivalent circuit models for design process of the proposed wideband filtering balun. (a) Lumped element prototype using Richard's transformation. (b) Simplified one by combining the cascaded shunt inductors. (c) Transformation of two UE circuits. (d) Proposed one by absorbing the transformer n_2 into the load. (e) Proposed one by absorbing the transformer n_1 to obtain the final 3-th order non-redundant network.

$$L = Z_S \quad (3)$$

$$Z = 2Z_M. \quad (4)$$

C. EQUIVALENT CIRCUIT SIMPLIFICATION

Next, an equivalent physics-based circuit model is further developed for facilitating the synthesized design process. To synthesize all the element values of the transformed circuit using the Richard's theory, all redundant elements are appropriately combined to get the non-redundant circuit model. In the following, the detailed process of legitimate circuit transformation and simplification is described as illustrated in Fig. 5(a)-(d) under the condition that the essence of the original circuit in frequency domain is maintained in transformation to its corresponding non-redundant circuit form.

By combining two middle shunt inductors together as one, the transformed circuit can be gained as shown in Fig. 5(b)

with the following transformation equation

$$L_1 = \frac{1}{2}L. \tag{5}$$

The ABCD-matrices of the left- and right-side circuit parts in Fig.5(c) can be derived in (6) and (7), respectively

$$\begin{aligned} & \frac{1}{\sqrt{1-t^2}} \begin{vmatrix} \frac{1}{n_2} & 0 \\ 0 & n_2 \end{vmatrix} \begin{vmatrix} 1 & Zt \\ \frac{t}{Z} & 1 \end{vmatrix} \\ &= \frac{1}{\sqrt{1-t^2}} \begin{vmatrix} \frac{1}{n_2} & Zt \\ \frac{n_2 t}{Z} & n_2 \end{vmatrix}, \tag{6} \end{aligned}$$

$$\begin{aligned} & \frac{1}{\sqrt{1-t^2}} \begin{vmatrix} \frac{t}{Z_1} & Z_1 t \\ 1 & 1 \end{vmatrix} \begin{vmatrix} \frac{1}{n_2} & 0 \\ 0 & n_2 \end{vmatrix} \\ &= \frac{1}{\sqrt{1-t^2}} \begin{vmatrix} \frac{1}{n_2} & n_2 Z_1 t \\ \frac{n_2 t}{Z_1 n_2} & n_2 \end{vmatrix}. \tag{7} \end{aligned}$$

Under the identical transmission property, (6) must be equal to (7) so as to determine the transformed parameter as

$$Z_1 = \frac{Z}{n_2^2}. \tag{8}$$

Then, by shifting and absorbing the transformer's turn ratio n_2 into the load as shown in Fig. 5(d), we can get

$$R_1 = \frac{2R}{n_2^2}. \tag{9}$$

Similarly, by shifting and absorbing n_1 into the load as shown in Fig. 5(e) and scaling the parameter values in the right side, the updated element values can be achieved as

$$L_2 = n_1^2 L_1, \tag{10}$$

$$Z_2 = n_1^2 Z_1, \tag{11}$$

$$R_2 = n_1^2 R_1. \tag{12}$$

D. SYNTHESIS PROCEDURE

Next, a distributed network consisting of transmission line sections with commensurate length can be treated as a lumped network and its performance can be analyzed and synthesized by the Richard's theory using the frequency transformation:

$$t = j \tan\left(\frac{\pi f}{2f_0}\right). \tag{13}$$

where t is the complex frequency variable in Richards domain, f_0 is the commensurate frequency at which all of the transmission-lines have the lengths equal to one quarter-wavelength, and f is the real frequency variable. In other words, the proposed balun can achieve a bandpass response at the central frequency of f_0 .

According to the relationship between the transmission coefficient and the filtering function, the square magnitude of transmission coefficient can be defined as

$$|S_{21}(t)|^2 = \frac{1}{1 + (\epsilon F_N)^2}. \tag{14}$$

where F_N is the n -th order filtering function and ϵ is the specified equal-ripple factor in the passband.

The ripple factor, the required ϵ and square magnitude of filtering function F_N can be expressed as

$$\epsilon^2 = 10^{\frac{LA}{10}} - 1 \tag{15}$$

$$|F_N|^2 = \left[T_m\left(\frac{t_C}{t}\right) T_n\left(\frac{\sqrt{1-t_C^2}}{\sqrt{1-t^2}}\right) - U_m\left(\frac{t_C}{t}\right) U_n\left(\frac{\sqrt{1-t_C^2}}{\sqrt{1-t^2}}\right) \right]^2. \tag{16}$$

where $t_c = j \tan(\pi f_c / 2f_0)$, f_c is the cutoff frequency that is used to determine the bandwidth of operation and $T_m(t) = \cos(mt \cos^{-1} t)$ is the m th-order Chebyshev polynomial of the first kind, $U_n(t) = \sin(ns \sin^{-1} t)$ is the n -th order degree unnormalized Chebyshev polynomial of the second kind, and m and n denote the number of high-pass ladder circuits element and UE element, respectively. Once the number of high-pass elements, i.e., series capacitors and shunt inductors, return loss, and bandwidth are specified, we can derive the transfer function. The order of filtering function should meet the following condition

$$N = m + n. \tag{17}$$

where N is the order of the filtering balun and the total number of circuit elements.

Using the energy conservation for a lossless network, we can get

$$|S_{21}(t)|^2 + |S_{11}(t)|^2 = 1. \tag{18}$$

The square of the magnitude of the reflection transfer function can be derived as

$$|S_{11}(t)|^2 = \frac{(\epsilon F_N)^2}{1 + (\epsilon F_N)^2}. \tag{19}$$

Consequently, we can find

$$|S_{11}(t)|^2 = S_{11}(t)S_{11}(-t). \tag{20}$$

Based on the relationship between S_{11} and Z_{in} under a normalized source resistance, the input impedance can be derived as

$$Z_{in} = \frac{1 + S_{11}(t)}{1 - S_{11}(t)}. \tag{21}$$

Therefore, the UE value can be found using the Richard's theorem [20].

$$Z_{UE,in}(t) = Z_{in}(1). \tag{22}$$

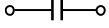
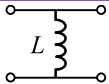
where the $Z_{UE,in}$ is the normalized characteristic impedance and $Z_{in}(1)$ is the input impedance looking from the UE element. The new input impedance of the remaining network after removing the UE can be written as

$$Z'_{in} = Z_{in}(1) \frac{tZ_{in}(1) - Z_{in}(t)}{tZ_{in}(t) - Z_{in}(1)}. \tag{23}$$

What's more, the values of the first series capacitor C and second shunt inductor L can be determined by the pole

removing technique as illustrated in Table 1 [21], [22]. So far, all the circuit values can be exactly synthesized. In all, if the input impedance of the two-port network can be derived from the specified transfer function, we can apply the Richards' theorem to determine the value of the cascaded transmission line, known as an UE, and apply the pole removing technique to find the LC values.

TABLE 1. Element extraction using the pole removing method.

Element	Z(t) or Y(t)	Pole	Value
	$Z(t) = \frac{1}{tC}$	$Z(t) _{t \rightarrow 0}$	$\frac{q_1}{p_0}$
	$Y(t) = \frac{1}{tL}$	$Y(t) _{t \rightarrow 0}$	$\frac{p_1}{q_0}$
$Z(t) = \frac{P(t)}{Q(t)} = \frac{p_n t^n + \dots + p_2 t^2 + p_1 t^1 + p_0}{q_n t^n + \dots + q_2 t^2 + q_1 t^1 + q_0}$			

III. SYNTHESIS FOR PARAMETRIC DETERMINATION

In this section, the claimed features will be demonstrated to confirm the effectiveness of the proposed method by following the design procedure outlined in Section II. To explain the circuit model based on the synthesis procedure, a triple-mode wideband filtering balun with $N = 3$, $f_o = 2.9$ GHz, and a fractional bandwidth of 110% will be designed herein, and a return loss level of 18 dB corresponds to $\varepsilon = 0.12690$. Substituting the specifications into (16), the square magnitude of the filtering function F_3 can be obtained

$$|F_3|^2 = \frac{9.14002t^4 + 19.13478t^2 + 10.01474}{-t^6 + t^4}. \quad (24)$$

By substituting the calculated values F_3 and ε into (19), the square magnitude of the reflection function can be expressed as following

$$|S_{11}|^2 = \frac{-0.147192t^4 - 0.30815t^2 - 0.16127}{t^6 - 1.14719t^4 - 0.30815t^2 - 0.16127}. \quad (25)$$

With (20), we choose the left-hand plane poles to be associated with S_{11} . The polynomial of the input reflection coefficient is deduced as

$$S_{11} = \frac{0.38365t^2 + 0.40159}{t^3 + 1.84109t^2 + 1.07188t + 0.40159}. \quad (26)$$

After appropriate arrangement, we can get the input port impedance of function of t by (21) as

$$Z_{in} = \frac{t^3 + 2.19775t^2 + 1.07188t + 0.80319}{t^3 + 1.43044t^2 + 1.07188t}. \quad (27)$$

Thus, the series capacitor can be determined by the pole removing method as elaborated in the Table. I

$$C_1 = 1.33452. \quad (28)$$

Meanwhile, the input impedance of the remaining network can be written as

$$Z'_{in} = \frac{t^3 + 1.44842t^2}{t^3 + 1.43044t^2 + 1.07188t}. \quad (29)$$

Similarly, the pole removing technique can be used to extract the shunt inductor as

$$L_2 = 1.35128. \quad (30)$$

So, the input impedance of remaining network becomes

$$Z''_{in} = \frac{t^3 + 1.44842t^2}{t^3 + 0.69040t^2}. \quad (31)$$

The Richard's theory is utilized to determine Z_2 using (22)

$$Z_1 = 1.44876. \quad (32)$$

Using (23) [19], the load impedance can be accordingly got

$$R_2 = 2.09792. \quad (33)$$

The ratio of two turn ratios can be determined as

$$\frac{n_1^2}{n_2^2} = 0.95332. \quad (34)$$

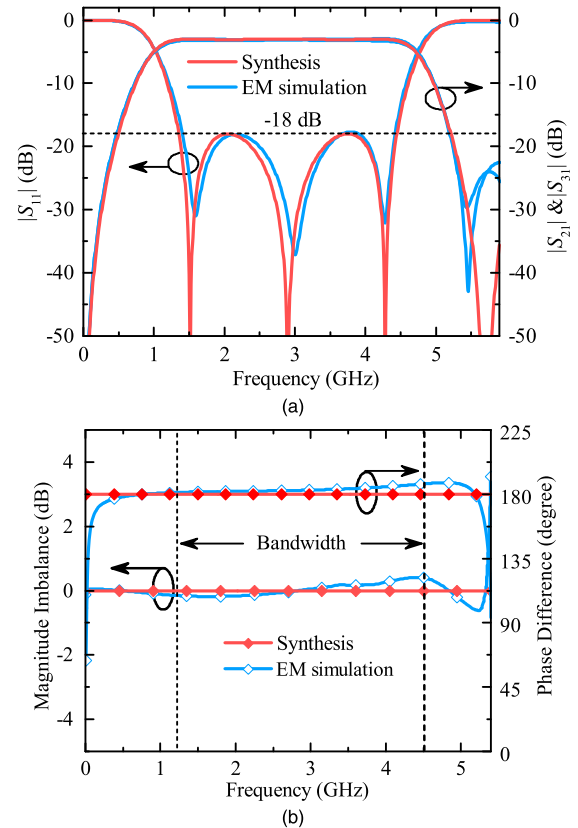
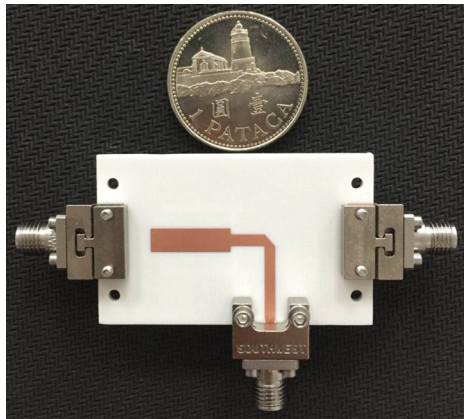
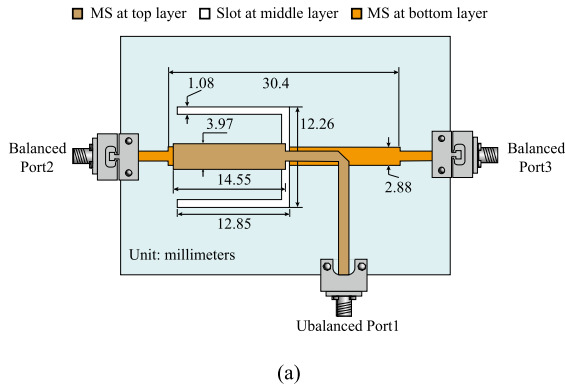
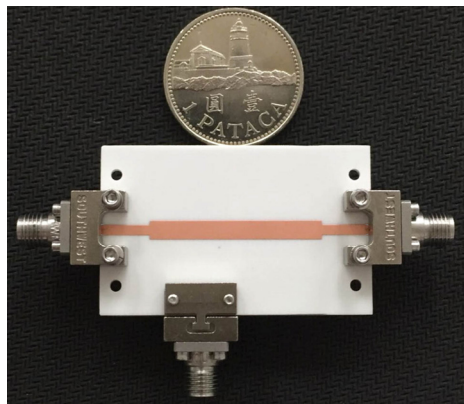


FIGURE 6. Synthesized and EM simulated results of the proposed filtering balun with center frequency at 2.9 GHz, 110% fractional bandwidth and 18-dB in-band return loss. (a) Frequency responses of S-parameters. (b) Magnitude imbalance and phase difference.



(b)



(c)

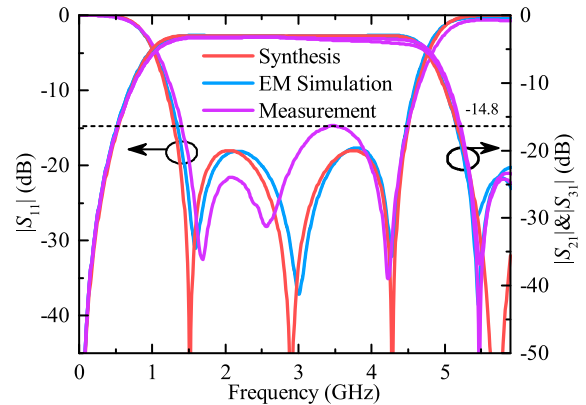
FIGURE 7. Layout and photographs of the proposed wideband filtering balun. (a) Layout with the key dimensions labeled. (b) and (c) Top-and bottom-view photographs of the fabricated filtering balun.

Considering the real situation in fabrication, $n_1 = 0.39264$, $n_2 = 0.66152$ are readily selected. Thus, the impedance of transmission line in Fig. 3 can be determined as

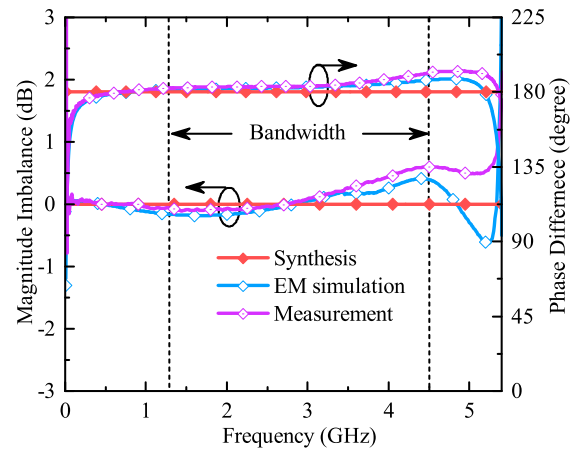
$$Z_O = 29.20 \Omega \quad (35)$$

$$Z_S = 128.82 \Omega \quad (36)$$

$$Z_M = 34.45 \Omega. \quad (37)$$



(a)



(b)

FIGURE 8. Comparison among the theoretical, EM simulated and measured results of the proposed wideband filtering balun. (a) Frequency responses of S-parameters. (b) Magnitude imbalance and phase difference.

Fig. 6(a) gives the theoretical and EM simulated magnitudes of S-parameters of the filtering balun by using the synthesized function and its equivalent circuit model in Fig. 3, respectively. The synthesized and simulated frequency responses are both plotted in Fig. 6(a) for comparison. It is noted that good agreement between the two sets of results is achieved over a wide frequency range up to 5.9 GHz. The simulated results in Fig. 6(a) show that more than 110% bandwidth for the return loss of better than 17.8 dB across the whole frequency band can be achieved, and three transmission poles can be observed in the passband. In addition, the synthesized and EM simulated magnitude imbalance and phase difference are plotted in Fig. 6(b). Again, the two sets of results are found in good agreement with each other in a wide band frequency range. It can be confirmed that the proposed filtering balun can be designed in a deterministic manner, thus validating the effectiveness of the proposed method.

IV. FABRICATION AND EXPERIMENTAL VERIFICATION

To further verify the proposed design method, the design procedure outlined in Section IV is applied to design a prototype circuit of the proposed filtering balun. Then,

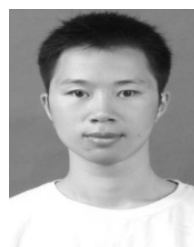
such a filtering balun circuit is fabricated and measured. The filtering balun prototype is implemented on the Rogers RO4003C substrate with a thickness of 0.813mm and a dielectric constant of 3.55. Realizable geometrical parameters are provided in Fig. 7(a). The top- and bottom-view photographs of the fabricated balun circuit are shown in Fig. 7(b) and (c), respectively. The simulated results are derived by a commercial full-wave simulator, Ansoft HFSS, and the measured ones are obtained by using the four-port vector network analyzer (VNA), R&S ZNB20. Consequently, the synthesized, EM simulated, and measured magnitudes of the reflection and transmission coefficients are superimposed in Fig. 8(a), showing good agreement with each other. These results indicate that the implemented filtering balun operates at the central frequency of 2.95 GHz with a fractional bandwidth of 109%. The measured in-band return loss is better than 14.8 dB and the insertion loss is superior to 0.9 dB. The synthesized, EM simulated, and measured of the magnitude imbalance and phase difference are superimposed in Fig. 8(b), showing good agreement with each other as well. As illustrated in Fig. 8(b), the proposed filtering balun exhibits good balanced performance with a magnitude imbalance less than 1.0 dB and a phase difference better than 9° over a wide band frequency range as depicted in Fig. 8(b). Thus, the proposed filtering balun not only exhibits sharp frequency selectivity, but also good magnitude imbalance and phase difference within the prescribed passband as always desired.

V. CONCLUSION

In this paper, a direct synthesis method has been presented for design of filtering balun on a proposed compact triple-mode using stacked composing resonators. More importantly, the frequency response of this filtering balun can be efficiently synthesized to meet the given design specifications. Next, a wideband filtering balun is designed using the proposed synthesis approach. To validate the proposed concept, a prototype balun circuit are designed and fabricated. Good agreement among three sets of frequency responses from the theoretical synthesis, EM simulation and measurement is obtained. It is our belief that the proposed synthesis technique is powerful in design of a variety of wideband filtering baluns and other microwave circuits.

REFERENCES

- [1] L. K. Yeung and K.-L. Wu, "An integrated RF balanced-filter with enhanced rejection characteristics," in *IEEE MTT-S Int. Microw. Symp. Dig.*, vol. 2, Jun. 2005, pp. 713–716.
- [2] Y.-X. Guo, Z. Y. Zhang, L. C. Ong, and M. Y. W. Chia, "A novel LTCC miniaturized dualband balun," *IEEE Microw. Wireless Compon. Lett.*, vol. 16, no. 3, pp. 143–145, Mar. 2006.
- [3] G. Zhang, J. Wang, J. Pan, and H. Gu, "Compact 60 GHz LTCC balun bandpass filter with two transmission zeroes," *Electron. Lett.*, vol. 51, no. 8, pp. 637–638, Apr. 2015.
- [4] G. Q. Zhang, J. X. Chen, J. Shi, H. Tang, H. Chu, and Z. H. Bao, "Design of multilayer balun filter with independently controllable dual passbands," *IEEE Microw. Wireless Compon. Lett.*, vol. 25, no. 1, pp. 10–12, Jan. 2015.
- [5] H. Tang, J.-X. Chen, H. Chu, G.-Q. Zhang, Y.-J. Yang, and Z.-H. Bao, "Integration design of filtering antenna with load-insensitive multilayer balun filter," *IEEE Trans. Compon., Packag., Manuf. Technol.*, vol. 6, no. 9, pp. 1408–1416, Sep. 2016.
- [6] E.-Y. Jung and H.-Y. Hwang, "A balun-BPF using a dual mode ring resonator," *IEEE Microw. Wireless Compon. Lett.*, vol. 17, no. 9, pp. 652–654, Sep. 2007.
- [7] P. Cheong, T.-S. Lv, W.-W. Choi, and K.-W. Tam, "A compact microstrip square-loop dual-mode balun-bandpass filter with simultaneous spurious response suppression and differential performance improvement," *IEEE Microw. Wireless Compon. Lett.*, vol. 21, no. 2, pp. 77–79, Feb. 2011.
- [8] S. Sun and W. Menzel, "Novel dual-mode balun bandpass filters using single cross-slotted patch resonator," *IEEE Microw. Wireless Compon. Lett.*, vol. 21, no. 8, pp. 415–417, Aug. 2011.
- [9] S. S. Gao and S. Sun, "Compact dual-mode balun bandpass filter with improved upper stopband performance," *Electron. Lett.*, vol. 47, no. 23, pp. 1281–1283, Nov. 2011.
- [10] F. Huang, J. Wang, and L. Zhu, "A new approach to design a microstrip dual-mode balun bandpass filter," *IEEE Microw. Wireless Compon. Lett.*, vol. 26, no. 4, pp. 252–254, Apr. 2016.
- [11] L. K. Yeung and K. L. Wu, "A dual-band coupled-line balun filter," *IEEE Trans. Microw. Theory Techn.*, vol. 55, no. 11, pp. 2406–2411, Nov. 2007.
- [12] C.-Y. Liou and S.-G. Mao, "Triple-band marchand balun filter using coupled-line admittance inverter technique," *IEEE Trans. Microw. Theory Techn.*, vol. 61, no. 11, pp. 3846–3852, Nov. 2013.
- [13] J. Wang, F. Huang, L. Zhu, C. Cai, and W. Wu, "Study of a new planar-type balun topology for application in the design of balun bandpass filters," *IEEE Trans. Microw. Theory Techn.*, vol. 64, no. 9, pp. 2824–2832, Sep. 2016.
- [14] C. Chai, J. Wang, L. Zhu, and W. Wu, "A new approach to design microstrip wideband balun bandpass filter," *IEEE Microw. Wireless Compon. Lett.*, vol. 26, no. 2, pp. 116–118, Feb. 2016.
- [15] T. Yang, M. Tamura, and T. Itoh, "Compact hybrid resonator with series and shunt resonances used in miniaturized filters and balun filters," *IEEE Trans. Microw. Theory Techn.*, vol. 58, no. 2, pp. 390–402, Feb. 2010.
- [16] C.-H. Wu, C.-H. Wang, S.-Y. Chen, and C. H. Chen, "Balanced-to-unbalanced bandpass filters and the antenna application," *IEEE Trans. Microw. Theory Techn.*, vol. 56, no. 11, pp. 2474–2482, Nov. 2008.
- [17] W. Feng and W. Che, "Wideband balun bandpass filter based on a differential circuit," in *IEEE MTT-S Int. Microw. Symp. Dig.*, Jun. 2012, pp. 1–3.
- [18] Y.-W. Lin, J.-C. Lu, and C.-Y. Chang, "Design of high-order wideband planar balun filter in S-plane bandpass prototype," *IEEE Trans. Microw. Theory Techn.*, vol. 60, no. 7, pp. 2124–2130, Jul. 2012.
- [19] J.-S. Hong and M. J. Lancaster, *Microstrip Filters for RF/Microwave Applications*. New York, NY, USA: Wiley, 2001.
- [20] P. I. Richards, "General impedance—Function theory," *Quart. Appl. Math.*, vol. 6, no. 1, pp. 21–29, 1948.
- [21] H. Orchard and G. Temes, "Filter design using transformed variables," *IEEE Trans. Circuit Theory*, vol. CT-15, no. 12, pp. 385–408, Dec. 1968.
- [22] M. C. Horton and R. J. Wenzel, "General theory and design of optimum quarter-wave TEM filters," *IEEE Trans. Microw. Theory Techn.*, vol. MTT-13, no. 5, pp. 316–327, May 1965.



LIN-PING FENG received the M.E. degree from the University of Electronic Science and Technology of China, Chengdu, China, in 2015. He is currently pursuing the Ph.D. degree. His current research interests include filter, antennas, and millimeter-wave antenna.



LEI ZHU (S'91–M'93–SM'00–F'12) received the B.Eng. and M.Eng. degrees in radio engineering from Southeast University, Nanjing, China, in 1985 and 1988, respectively, and the Ph.D. degree in electronic engineering from the University of Electro-Communications, Tokyo, Japan, in 1993.

From 1993 to 1996, he was a Research Engineer with Matsushita-Kotobuki Electronics Industries Ltd., Tokyo. From 1996 to 2000, he was a Research Fellow with the École Polytechnique de Montréal, Montréal, QC, Canada. From 2000 to 2013, he was an Associate Professor with the School of Electrical and Electronic Engineering, Nanyang Technological University, Singapore. He joined the Faculty of Science and Technology, University of Macau, Macau, China, as a Full Professor, in 2013, where he has been the Head of Department of electrical and computer engineering since 2014 and a Distinguished Professor since 2016. He has authored or co-authored over 375 papers in international journals and conference proceedings. His research interests include microwave circuits, guided-wave periodic

structures, planar antennas, and computational electromagnetic techniques. His papers have been cited more than 4460 times with the H-index of 37 (source: ISI Web of Science).

Dr. Zhu served as a member for the IEEE MTT-S Fellow Evaluation Committee from 2013 to 2015 and has been serving as a member for the IEEE AP-S Fellows Committee since 2015. He was a recipient of the 1997 Asia-Pacific Microwave Prize Award. He received the 1996 Silver Award of Excellent Invention from Matsushita-Kotobuki Electronics Industries Ltd. and the 1993 First-Order Achievement Award in Science and Technology from the National Education Committee, China. He was the Associate Editor of the IEEE Transactions on Microwave Theory and Techniques from 2010 to 2013 and the IEEE Microwave and Wireless Components Letters from 2006 to 2012. He served as the General Chair for the 2008 IEEE MTT-S International Microwave Workshop Series on the Art of Miniaturizing RF and Microwave Passive Components, Chengdu, China, and the Technical Program Committee Co-Chair for the 2009 Asia-Pacific Microwave Conference, Singapore.

• • •